Crossing Bifurcations and Unstable Dimension Variability

K. T. Alligood and E. Sander
Mathematical Sciences, George Mason University, Fairfax, Virginia 22030, USA

J. A. Yorke
IPST, University of Maryland, College Park, Maryland 20742, USA

(Received 14 April 2004; published 23 June 2006)

A crisis is a global bifurcation in which a chaotic attractor has a discontinuous change in size or suddenly disappears as a scalar parameter of the system is varied. In this Letter, we describe a global bifurcation in three dimensions which can result in a crisis. This bifurcation does not involve a tangency and cannot occur in maps of dimension smaller than 3. We present evidence of unstable dimension variability as a result of the crisis. We then derive a new scaling law describing the density of the new portion of the attractor formed in the crisis. We illustrate this new type of bifurcation with a specific example of a three-dimensional chaotic attractor undergoing a crisis.

DOI: 10.1103/PhysRevLett.96.244103 PACS numbers: 05.45.Ac, 05.40.−a

Introduction.—Crises of chaotic attractors are probably the most easily observed and most often described global bifurcations. Descriptions and analysis of crises for two-dimensional systems began in the early 1980's [1]. Typically, these descriptions involved the structure of underlying stable and unstable manifolds of periodic saddles in the attractor. Experimental studies followed, and within a decade, numerical invariants and methods of quantifying crises were developed. For example, in [2,3] magnoelastic ribbon experiments showed crisis-induced intermittency and confirmed the related theory of critical exponents. Models of laser systems continue to provide examples of chaotic attractors which undergo crises. Of particular current interest are experimental studies of semiconductor lasers with optical injection or optical feedback [4–6] and spatially coupled semiconductor laser arrays, (see [7] for crises occurring in a system of two coupled microchip lasers). Most of these examples are parametrized two-dimensional systems or projections onto one or two variables. For invertible two-dimensional maps, crises are observed to occur as a result of tangencies of stable and unstable manifolds of underlying saddle orbits in the attractor. In higher-dimensional maps such as the example presented here, crises can occur without tangencies. Figure 1(a) shows a chaotic attractor of a three-dimensional map, whose formula is given later. As a scalar parameter is varied, the system undergoes a *twisted crossing* bifurcation, and the attractor jumps discontinuously in size [Fig. 1(b)]. This bifurcation has not been previously described in the physics literature.

Unstable dimension variability.—A key difficulty which must be understood in modeling higher-dimensional dynamical systems is the phenomenon of unstable dimension variability (UDV): an attractor has UDV if it contains periodic orbits with different numbers of unstable directions. (See [8,9] for introductory papers.) With UDV, an attractor has a (finite time) Lyapunov exponent which can fluctuate around zero, causing computer generated trajectories to be unshadowable [10–12]. The first examples were typically of coupled chaotic systems that had symmetries and/or synchronization manifolds [13,14]. Among physical models displaying these phenomena is the analysis of UDV in the double rotor in [15]. A mechanism for the development of UDV in more general coupled systems is given in [12,16]. An example of a three-dimensional map with UDV appears in [17]; this example, however, is not the result of a crossing bifurcation. In the present Letter we demonstrate numerically that the attractor depicted in Fig. 1(b) has UDV.

Chaotic invariant sets are filled with fixed points and periodic point saddles (or repellers) whose stable and unstable manifolds cross in heteroclinic orbits. An invertible two-dimensional map cannot have an invariant set displaying UDV: in two dimensions, saddle points all have one unstable dimension. In three dimensions, however, there can be a heteroclinic connection between a saddle with a two-dimensional unstable manifold and a saddle with a one-dimensional unstable manifold. The attractor in

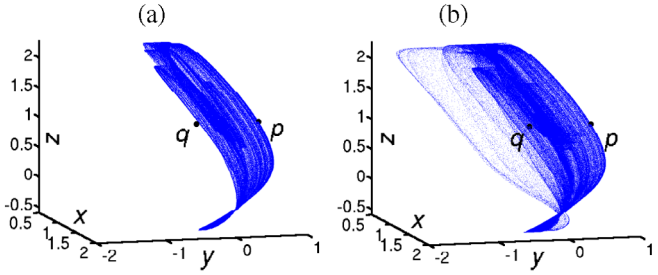

FIG. 1 (color online). The attractor for a crossing bifurcation as in Eq. (2) (a) before and (b) after the crisis. The bifurcation occurs at the parameter for which the fixed point q becomes part of the attractor. The jump in the size of the attractor is discontinuous with respect to parameter (but with small density, which then increases).

Fig. 1 has this type of heteroclinic connection throughout the parameter range shown.

Numerical verification of UDV using power laws.—In order to conclude that UDV occurs, we verify directly that two fixed points of different index are both contained within the attractor. This is done by verifying that the scaling of the probability distribution of the attractor near each fixed point agrees with the following analytical estimate for the *pointwise dimension*, similar in flavor to the Lyapunov dimension at a fixed point: For a fixed parameter, consider a fixed point saddle q having two unstable directions with corresponding eigenvalues $|\lambda_1|$, $|\lambda_2| > 1$ and one stable direction corresponding to $|\mu| < 1$. Starting with a unit box around the fixed point q, the probability $P(\epsilon)$ that a point enters a box of side length ϵ is approximately $\epsilon^2(\lambda_1\lambda_2)^{-k}$, where $\mu^k = \epsilon$. Thus with two unstable directions, the pointwise dimension is $\log P(\epsilon)/\log\epsilon = 2 + (\log|\lambda_1| + \log|\lambda_2|)/|\log|\mu||$. Similarly, for a saddle fixed point p with eigenvalues $|\alpha| > 1$, $|\beta_1| < |\beta_2| < 1$, $\log P(\epsilon)/\log\epsilon = 1 + \log|\alpha|/|\log|\beta_2||$.

Figure 2 shows that there is good agreement between the pointwise dimension and the computed probability distribution for the attractor near each of the two fixed points.

We have chosen to use a direct route for verifying UDV rather than the more common method of computing fluctuations near zero in finite time Lyapunov exponents. For one thing, since we possess detailed information about the topology of the example, a direct method is straightforward. More fundamentally, for η near the bifurcation value, the density of the global attractor is small near the fixed point q (see the discussion below), meaning that for long orbits, the behavior at p dominates, forcing the middle Lyapunov exponent to be negative. For our example, if $-0.4 < \eta < 0$, and the total orbit length is $M = 10^8$, then

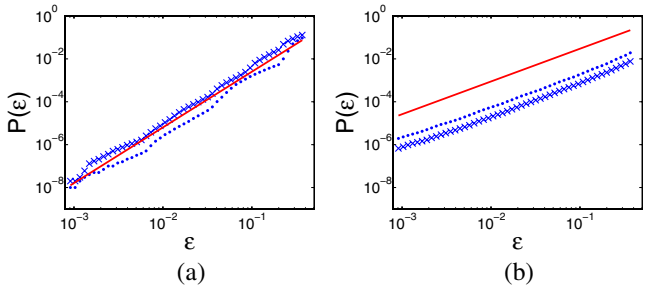

FIG. 2 (color online). The scaling of the fraction $P(\epsilon)$ of the attractor points near fixed points (a) q and (b) p for the system in Eq. (2). The dots and crosses are shown for $\eta = -0.2625$ and $\eta = -0.1525$, respectively. The slopes of the lines in (a) (using ten values of η) are 2.78 ± 0.3. The error comes from a combination of mismatch in the linear fit and global fluctuations with respect to the parameter. The scaling predicted using power laws is plotted with a solid line. The slope is 2.599, with variation of 0.003 as η varies (hence only one line is plotted). After removing transient behavior, an orbit of length 10^8 was used. Similarly, in (b), $P(\epsilon)$ has slope is 1.57 ± 0.1 with prediction 1.52 ± 0.01.

the calculated maximum length (denoted by T) of a subset of this long orbit with positive finite time Lyapunov exponent is around 30. This is not surprising: Any orbit Ω with positive finite time middle Lyapunov exponent must be near p and q in proportion to the relative strengths of the middle Lyapunov exponents of q and p. In our example, $L_p \approx -1$ and $L_q \approx 0.5$. Thus Ω comes near q twice as often as near p. However, the calculation above shows that on average orbits stay near p longer than near q. By a rough calculation, in a length 10^8 orbit in the attractor, the orbit is expected to stay close to q for a maximum of $\log(10^8)/\log(\lambda_1\lambda_2) = 18$ consecutive iterates, meaning $T \approx 27$. For larger T the problem is not computationally feasible. For example, we predict that for $T \approx 100$, we would need $M \approx 10^{45}$.

This low density near the second fixed point is always present for a crossing bifurcation, but is not limited to this case. We conjecture that detection of UDV via Lyapunov exponents will miss many cases in which UDV is present. We believe that this is the first example clearly demonstrating the distinction between the definition of UDV and feasible computation of UDV using Lyapunov exponents fluctuating near zero.

A new scaling law for attractor density.—We have developed a new power law for the scaling of the density of the new part of the attractor after the crisis occurs. Let A_{old} be the chaotic attractor prior to the bifurcation point, and let A_{new} be the new part of the attractor that only appears after the bifurcation. Let τ be the number of iterates within A_{old} between visits to A_{new}. For a particular orbit, τ varies sensitively on initial conditions. However, one typically sees an exponential probability distribution of the form $P(\tau) \propto K^{-1}\exp(-\tau/K)$, for large τ where K is the mean transient length [1]. This has been verified for our numerical example. In the planar case, it was shown in the 1980's that the mean lifetime $K = K(\eta)$ as a function of the parameter η is a power law. The power law for planar crises occurring as a result of both homoclinic and heteroclinic tangencies was established by Grebogi *et al.* [1]. Figure 3 shows that for the example of a crossing bifurcation given here, $K(\eta)$ exhibits power law behavior. However, since a crossing cycle is a nontangency bifurcation, the relationship between the slope of this line is not given by the traditional two-dimensional equations. Our new power law is based on the geometry of the three-dimensional bifurcation, as we now describe: The function $K(\eta) = \eta^\gamma$. The exponent γ is given by

$$\gamma = 1 + \frac{\log|\lambda_1|}{\log|\lambda_2|} + \frac{\log|\alpha|}{\log|\beta_2|}, \tag{1}$$

where $|\lambda_1| > |\lambda_2| > 1 > |\mu|$ and $|\alpha| > 1 > |\beta_2| > |\beta_1|$ are the eigenvalues for the fixed points q and p, respectively. The derivation of this scaling law will appear in another paper. The comparison between prediction and computed values is shown in Fig. 3.

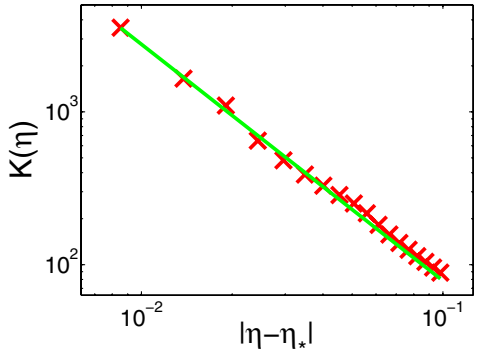

FIG. 3 (color online). The mean number of iterates K remaining in A_{old} (as defined in the text) prior to entering A_{new} as a function of $|\eta - \eta_*|$. For a crossing bifurcation, $K(\eta)$ obeys a power law. The bifurcation point $\eta_* = -0.1320$ is found by optimizing the linear fit. After removing transient behavior, an orbit of length 10^7 was used. The solid line shows the scaling law from Eq. (1). The slope of the line fitting the numerical data is -1.50 ± 0.06. The predicted slope is -1.55 with a fluctuation of 0.01 as η varies.

Geometry of crossing bifurcations.—An interesting distinction between a two-dimensional and a three-dimensional ambient space is the nature of heteroclinic orbits at crossings of stable and unstable manifolds. Such crossings in two-dimensional maps result generically in isolated heteroclinic points. (A planar map with a connected segment of heteroclinic points can be perturbed to one with isolated heteroclinic points.) In three-dimensional maps, two two-dimensional invariant manifolds can intersect in a 1D curve which cannot be perturbed away. See Fig. 4, in which p and q are hyperbolic fixed points with one-dimensional unstable manifold $U(p)$ and one-dimensional stable manifold $S(q)$, respectively. The two-dimensional unstable manifold of q, $U(q)$, intersects the two-dimensional stable manifold of p, $S(p)$. We refer to the 1D curve of heteroclinic points as a *connecting arc*.

The configuration of Fig. 5 depicts a global bifurcation that occurs at η_*, at which $U(p)$ intersects $S(q)$ at the point k [Fig. 5(b)]. Note that the intersection is not a tangency. For $\eta < \eta_*$, $U(p)$ is to the right of $S(q)$ [Fig. 5(a)]. For $\eta > \eta_*$, $U(p)$ is to the left of $S(q)$ [Fig. 5(c)]. Any nearby one-parameter family exhibits the same phenomena. It is this construction that we call a *crossing bifurcation*. A crossing bifurcation only occurs in a system with periodic orbits with different numbers of unstable directions.

Two types of crossing bifurcations.—The type of crisis occurring at a crossing bifurcation depends on more global properties: in particular, it depends on whether the manifold $U(p)$ is twisted or not. If $U(p)$ is not twisted, as illustrated in Fig. 6(a), then for $\eta < \eta_*$, there are both homoclinic points to p and homoclinic points to q; for $\eta > \eta_*$, there are none. Diaz *et al.* [18,19] analyzed the untwisted case and showed that there is UDV for a large set of parameters prior to bifurcation, depending on the particular choice of generic maps.

If $U(p)$ twists around $U(q)$ [Fig. 6(b)], then $U(q)$ crosses $S(p)$ near k, for $\eta < \eta_*$, resulting in recurrent behavior before the bifurcation. In the example, the fixed point q is not in the chaotic attractor. There is a chaotic attractor containing p in this parameter range which then undergoes a crisis at η_*. After the bifurcation, $U(q)$ continues to cross $S(p)$, and now also crosses $S(q)$. The codimension two orbit flip bifurcation of vector fields [20] has a similar twisting of manifolds to the crossing bifurcation; however, the orbit flip is a homoclinic bifurcation and is thus not related to UDV.

An example of a crossing bifurcation.—The following is an example of a twisted crossing bifurcation. The three-dimensional map is of the form

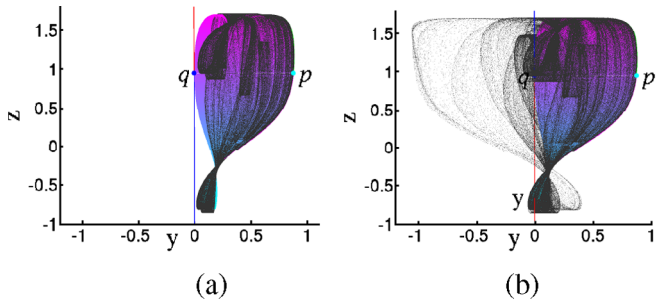

FIG. 4 (color online). A crossing bifurcation is characterized by the fact that A_{old} lies in a strip of the two-dimensional manifold $U(q)$ bounded by the one-dimensional unstable manifold $U(p)$ and the strong unstable manifold of q. The manifolds and attractor for the system in Eq. (2) are shown (a) prior to bifurcation and (b) after bifurcation. The point y is the first intersection of $U(p)$ and $S(q)$. $S(p) \cap U(q)$ includes the line segment connecting q to p. [$S(p)$ is not shown.] Color corresponds to the z coordinate.

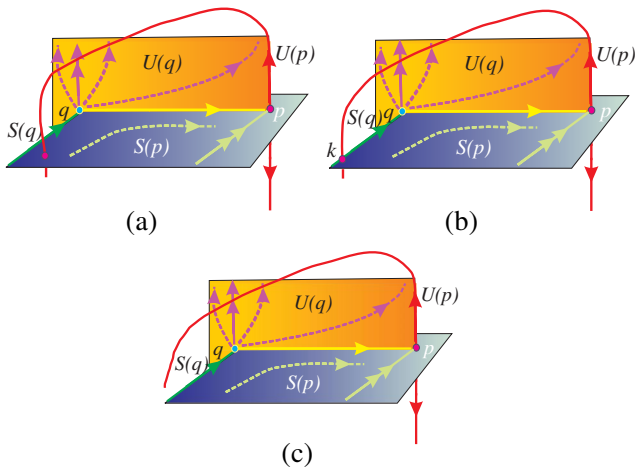

FIG. 5 (color online). The geometry of a crossing bifurcation. As a bifurcation parameter η varies, the curve $U(p)$ crosses the curve $S(q)$ from right to left.

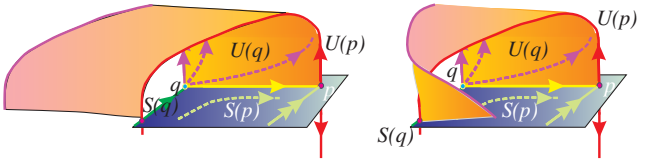

(a) (b)

FIG. 6 (color online). For a crossing bifurcation, the two-dimensional manifolds are either (a) untwisted or, (b) as in our example, twisted.

$$(x, y, z) \mapsto (h_1(x, z), G_\eta(x, y), h_2(x, z)), \tag{2}$$

where $h(x, z) = (2.12 - x^2 - 0.3z, x)$, is the two-dimensional Hénon map, chosen in a parameter regime where there is a saddle fixed point (x_1, z_1) with $x_1 = z_1 \approx 0.94\,452$ within the attractor, such that the unstable manifold of this fixed point limits to the entire Hénon attractor. That is, the projection of the global attractor to the xz plane is the Hénon attractor. Note that the line $CL = \{(x_1, y, z_1): y \in R\}$ is invariant. Fixed points p and q both lie on line CL and are thus of the form $p = (x_1, y_p, z_1)$, $q = (x_1, y_q, z_1)$. The line segment parallel to the y axis connecting p to q is constructed to be the connecting arc previously described. That is, restricting to CL, q is an unstable fixed point, and p is a stable fixed point. Between p and q orbits converge forwards to p and backwards to q. Far away from the line CL, $G_\eta(x, y)$ is constructed so that there is a twist in the unstable manifold strip between p and q. Specifically, $G_\eta(x, y) = g(y)[1 + \tanh(2x)]/2 + L_\eta(y)[1 - \tanh(2x)]/2$, where $g(y) = 1 - e^{-1.7y-y^2}$, and $L_\eta(y) = \eta + (1 - y)/3$.

Thus near CL, $G_\eta(x, y) \approx g(y)$, where $g(y)$ is has a stable and unstable fixed point with a connecting segment between them. Far from CL, $G_\eta(x, y) \approx L_\eta(y)$, where L_η is a linear function with negative slope. This has the effect of adding a twist to the unstable manifold, as shown in Fig. 4.

As the parameter η varies, the one-dimensional unstable manifold of p shifts. At the bifurcation parameter η_* the unstable manifold of p intersects the one-dimensional stable manifold of q. See Fig. 4.

J. A. Y. was partially supported by NSF Grant No. 0104087.

[1] C. Grebogi, E. Ott, and J. A. Yorke, Phys. Rev. Lett. **48**, 1507 (1982); Physica D (Amsterdam) **7**, 181 (1983); C. Grebogi, E. Ott, F. Romeiras, and J. A. Yorke, Phys. Rev. A **36**, 5365 (1987).
[2] J. C. Sommerer, William L. Ditto, Celso Grebogi, Edward Ott, and Mark L. Spano, Phys. Lett. A **153**, 105 (1991); Phys. Rev. Lett. **66**, 1947 (1991).
[3] W. L. Ditto, S. Rauseo, R. Cawley, C. Grebogi, G.-H. Hsu, E. Kostelich, E. Ott, H. T. Savage, R. Segnan, M. L. Spano, and J. A. Yorke, Phys. Rev. Lett. **63**, 923 (1989).
[4] S. Wieczorek, B. Krauskopf, and D. Lenstra, Phys. Rev. E **64**, 056204 (2001); Opt. Lett. **26**, 816 (2001).
[5] T. Heil, I. Fischer, W. Elsäßer, B. Krauskopf, K. Green, and A. Gavrielides, Phys. Rev. E **67**, 066214 (2003).
[6] R. Davidchack, Ying-Cheng Lai, Athanasios Gavrielides, and Vassilios Kovanis, Physica D (Amsterdam) **145**, 130 (2000).
[7] M. Moller, B. Forsmann, and W. Lange, Quantum Semiclass. Opt. **10**, 1 (1998).
[8] Y.-C. Lai, C. Grebogi, and J. Kurths, Phys. Rev. E **59**, 2907 (1999).
[9] E. Kostelich, I. Kan, C. Grebogi, E. Ott, and J. Yorke, Physica D (Amsterdam) **109**, 81 (1997).
[10] S. Dawson, C. Grebogi, T. Sauer, and J. A. Yorke, Phys. Rev. Lett. **73**, 1927 (1994).
[11] P. Moresco and S. P. Dawson, Phys. Rev. E **55**, 5350 (1997).
[12] T. D. Sauer, Phys. Rev. E **65**, 036220 (2002); Chaos **13**, 947 (2003).
[13] Y.-C. Lai and C. Grebogi, Phys. Rev. Lett. **82**, 4803 (1999).
[14] R. L. Viana and C. Grebogi, Phys. Rev. E **62**, 462 (2000).
[15] F. J. Romeiras, C. Grebogi, E. Ott, and W. P. Dayawansa, Physica D (Amsterdam) **58**, 165 (1992).
[16] E. Barreto and P. So, Phys. Rev. Lett. **85**, 2490 (2000).
[17] S. P. Dawson, Phys. Rev. Lett. **76**, 4348 (1996).
[18] L. J. Díaz and J. Rocha, Ergodic Theory Dynam. Syst. **21**, 25 (2001); Nonlinearity **10**, 857 (1997).
[19] L. J. Díaz and J. Rocha, Fund. Math. **174**, 127 (2002).
[20] B. Sandstede, Ph.D. thesis, University of Stuttgart, 1993; M. Kisaka, H. Kokubu, and H. Oka, J. Dyn. Differ. Equ. **5**, 305 (1993).